RESEARCH ARTICLE SUMMARY

AGING

Boosting neuronal activity-driven mitochondrial DNA transcription improves cognition in aged mice

Wenwen Li†, Jiarui Li†, Jing Li, Chen Wei, Tal Laviv, Meiyi Dong, Jingran Lin, Mariah Calubag, Lesley A Colgan, Kai Jin, Bing Zhou, Ying Shen, Haohong Li, Yihui Cui, Zhihua Gao, Tao Li, Hailan Hu, Ryohei Yasuda, Huan Ma*

INTRODUCTION: The dynamic coordination of energy and mass in the brain is essential for understanding cognitive function and its evolution with age. Mitochondria, the cell's energy hubs, contain their own genome (mtDNA), which encodes key components of oxidative phosphorylation (OXPHOS) that produces adenosine triphosphate to power neuronal and synaptic functions. However, how mitochondrial gene expression is regulated during information processing in the brain remains unclear. This question becomes particularly important with aging, as mtDNA levels in neurons decrease, coinciding with a decline in synaptic and neuronal functions.

RATIONALE: This study aims to investigate whether neuronal and synaptic excitation regulates mitochondrial gene expression in a transcription-dependent manner. If excitation-dependent mitochondrial gene transcription coupling (E-TC$_{mito}$) exists, what are the underlying mechanisms, and how does the regulation of this process, triggered by mental activity, affect brain functions such as synaptic transmission and memory? Given the decline in both synaptic function and mitochondrial integrity with advancing age, understanding E-TC$_{mito}$ could provide insights into the complex interplay between these key elements implicated in cognitive aging.

RESULTS: We demonstrate that neuronal and synaptic activity enhances mtDNA expression in excitatory neurons, a process mediated by activity-dependent mitochondrial calcium influx ([Ca^{2+}]$_{mito}$) and transcriptional control mechanisms involving mitochondrial Ca^{2+}-calmodulin–dependent protein kinase II (CaMKII$_{mito}$) and Ca^{2+}/cAMP response element–binding protein (CREB$_{mito}$). Specifically, neuronal activation induces the phosphorylation of the mitochondrial calcium uniporter (MCU) through CaMKII$_{mito}$ in an activity-dependent manner, thereby feedforward-regulating [Ca^{2+}]$_{mito}$. In turn, this activity-dependent process phosphorylates the transcription factor (TF) CREB$_{mito}$ to control mtDNA transcription and expression. Thus, E-TC$_{mito}$ repurposes molecules traditionally associated with excitation-transcription coupling in the nucleus (E-TC$_{nuc}$) to regulate mitochondrial DNA transcription, which can be specifically recruited in dendritic areas closely linked to synaptic activation. In both in vitro and in vivo models, blocking E-TC$_{mito}$ impaired activity-driven mtDNA expression and profoundly disrupted neuronal energy reserves, reducing the capacity to meet synaptic demands. This regulatory mechanism provides crucial feedback control to maintain synaptic resilience against activity challenges and plays an integral role in memory processes. Aged mice exhibited diminished activity-dependent mitochondrial calcium signaling and mtDNA expression, suggesting an age-related decline in E-TC$_{mito}$. Notably, expressing a constitutively active form of CREB$_{mito}$ in aged mice restored activity-dependent mtDNA expression, increased neuronal energy reserves, and enhanced memory performance, suggesting a potential strategy to mitigate age-related cognitive decline.

CONCLUSION: This study uncovers the critical role of E-TC$_{mito}$ in regulating mitochondrial gene expression in response to neuronal and synaptic activity and mental experiences, showing that E-TC$_{mito}$ functions differently from classic excitation-transcription coupling in the nucleus (E-TC$_{nuc}$). It highlights how age-dependent E-TC$_{mito}$ sustains neuronal energy reserves, maintains synaptic resilience, and supports memory by regulating mitochondria in an activity-driven manner. These findings suggest that targeting E-TC$_{mito}$ could offer a therapeutic approach to counteract age-related cognitive decline, opening valuable avenues for future research into brain aging and neurodegenerative diseases. ■

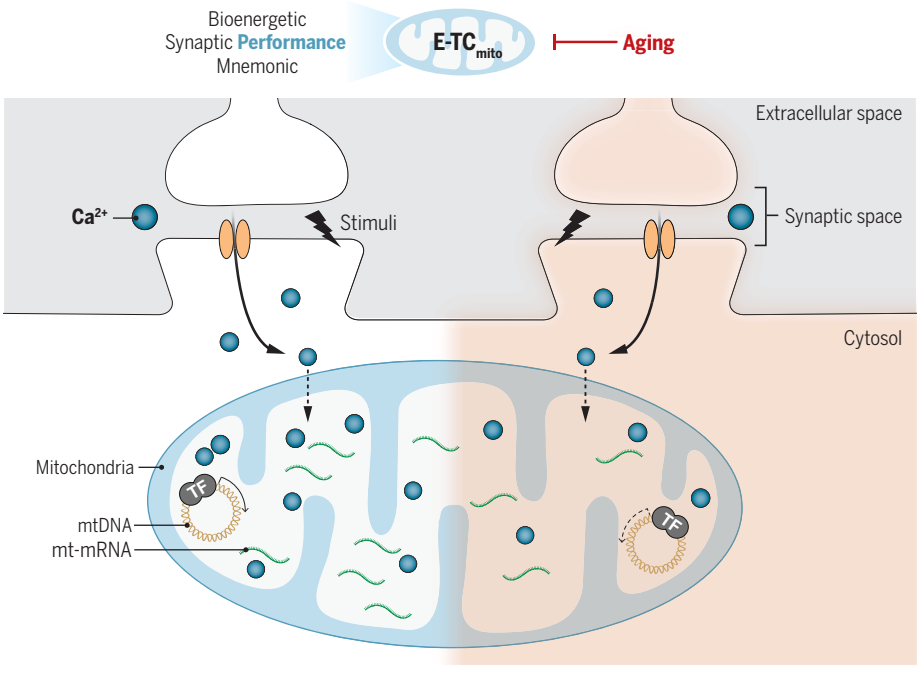

Linking mitochondrial gene transcription with mental activity through age-dependent E-TC$_{mito}$. During information processing, neuronal and synaptic excitation triggers mtDNA expression through mitochondrial calcium signaling, thereby sustaining synaptic transmission and memory functions. This use-dependent mitochondrial plasticity diminishes with age, contributing to age-related neurological deficits. Enhancing this process in aged animals has shown prospective benefits in mitigating memory decline, positioning it as a strategic target for combating cognitive aging.

The list of author affiliations is available in the full article online.
*Corresponding author. Email: mah@zju.edu.cn
†These authors contributed equally to this work.
Cite this article as W. Li *et al.*, *Science* **386**, eadp6547 (2024).
DOI: 10.1126/science.adp6547

READ THE FULL ARTICLE AT
https://doi.org/10.1126/science.adp6547

RESEARCH ARTICLE

AGING

Boosting neuronal activity-driven mitochondrial DNA transcription improves cognition in aged mice

Wenwen Li[1,2,3]†, Jiarui Li[1,2,3]†, Jing Li[1,2,3], Chen Wei[1,2,3], Tal Laviv[4,5], Meiyi Dong[1,2,3], Jingran Lin[1,2,3], Mariah Calubag[6,7], Lesley A Colgan[8], Kai Jin[1,2,3], Bing Zhou[9], Ying Shen[3], Haohong Li[3], Yihui Cui[3], Zhihua Gao[3], Tao Li[2,3], Hailan Hu[2,3,10], Ryohei Yasuda[8], Huan Ma[1,2,3,10]*

Deciphering the complex interplay between neuronal activity and mitochondrial function is pivotal in understanding brain aging, a multifaceted process marked by declines in synaptic function and mitochondrial performance. Here, we identified an age-dependent coupling between neuronal and synaptic excitation and mitochondrial DNA transcription (E-TC$_{mito}$), which operates differently compared to classic excitation-transcription coupling in the nucleus (E-TC$_{nuc}$). We demonstrated that E-TC$_{mito}$ repurposes molecules traditionally associated with E-TC$_{nuc}$ to regulate mitochondrial DNA expression in areas closely linked to synaptic activation. The effectiveness of E-TC$_{mito}$ weakens with age, contributing to age-related neurological deficits in mice. Boosting brain E-TC$_{mito}$ in aged animals ameliorated these impairments, offering a potential target to counteract age-related cognitive decline.

How mitochondria adapt their DNA expression to meet the dynamic energy needs of neuronal activity, especially as pronounced declines in mitochondrial DNA (mtDNA) in aging neurons signal an impending energy crisis in the brain (*1*, *2*), remains to be fully elucidated. Excitation-transcription coupling (E-TC) is the process by which neurons can change their transcriptional program through the actions of transcription factors in response to external stimuli (*3*–*5*). This use-dependent plasticity links neuronal excitation to de novo gene transcription in the nucleus (E-TC$_{nuc}$) (*6*–*8*), thus playing a fundamental role in supporting enduring synaptic plasticity and memory (*9*–*11*). Mitochondria, however, are distinct among extranuclear organelles in that they contain their own genetic system. In vertebrates, the mitochondrial genome consists of circular double-stranded mtDNA, which encodes essential subunits of oxidative phosphorylation (OXPHOS) that generate the cellular energy carrier adenosine triphosphate (ATP) to empower neuronal and synaptic functions (*12*–*15*). The essential role of mtDNA in the nervous system raises the critical question of whether, and how, synaptic and neuronal excitation can regulate its expression (E-TC$_{mito}$), potentially providing a key mechanism for use-dependent mitochondrial control in neurons (*16*, *17*).

Most of our understanding of activity-dependent mitochondrial gene regulation stems from extensive studies in non-neuronal excitable cells such as muscles, showing that the nuclear peroxisome proliferator–activated receptor-γ (PPARγ) coactivator-1α (PGC-1α) is a master transcription regulator of mitochondria (*16*). However, although PGC-1α is expressed in the developing brain, its expression is strongly reduced in excitatory neurons upon maturation (*18*). Furthermore, in contrast to muscle cells, excitatory neurons exhibit intricate morphologies characterized by highly polarized axonal and dendritic structures, which are capable of extending over considerable distance (*19*, *20*). This complex architecture, coupled with the short half-life of mitochondrial mRNAs (*21*), suggests a substantial advantage for the activity-dependent, localized expression of mitochondria-encoded genes within neurons. The potential importance of such a process is particularly pronounced in dendrites, where heightened OXPHOS-dependent bioenergetic resources are critical for supporting local postsynaptic transmission (*15*, *22*, *23*), and mitochondrial mobility is reduced compared to that in axons (*15*, *24*–*26*). Against this backdrop, we demonstrate that E-TC$_{mito}$ actively operates in the brain, directly linking neuronal activity with mtDNA transcription. Through the elucidation of key molecular constituents within the E-TC$_{mito}$ pathway, we identified a potential mechanism that could be leveraged for improving mitochondrial performance through experience- and activity-induced transcriptional governance of mtDNA expression, in particular in the aging brain.

[1]Department of Neurology of Second Affiliated Hospital and Liangzhu Laboratory, School of Brain Science and Brain Medicine, Zhejiang University School of Medicine, Hangzhou, China. [2]Affiliated Mental Health Center and Hangzhou Seventh People's Hospital, Zhejiang University School of Medicine, Hangzhou, China. [3]MOE Frontier Science Center for Brain Science and Brain-machine Integration, State Key Laboratory of Brain-machine Intelligence, NHC and CAMS Key Laboratory of Medical Neurobiology, Zhejiang University, Hangzhou, China. [4]Department of Physiology and Pharmacology, Faculty of Medical and Health Sciences, Tel Aviv University, Tel Aviv, Israel. [5]Sagol School of Neuroscience, Tel Aviv University, Tel Aviv, Israel. [6]Department of Medicine, University of Wisconsin-Madison, Madison, WI, USA. [7]William S. Middleton Memorial Veterans Hospital, Madison, WI, USA. [8]Department of Neuronal Signal Transduction, Max Planck Florida Institute for Neuroscience, Jupiter, FL, USA. [9]Beijing Advanced Innovation Center for Big Data-Based Precision Medicine, Beihang University, Beijing, China. [10]Research Units for Emotion and Emotion disorders, Chinese Academy of Medical Sciences, Beijing, China.
*Corresponding author. Email: mah@zju.edu.cn
†These authors contributed equally to this work.

Synaptic and neuronal activity boosts mitochondrial DNA expression

To assess the recruitment of E-TC$_{mito}$ by synaptic and neuronal activity, we activated neurons in acute hippocampal slices by blocking inhibitory synapses with the specific γ-aminobutyric acid type A ($GABA_A$) receptor antagonist picrotoxin (PTX, 50 μM, 1 hour), thereby enhancing excitatory synaptic transmission and neuronal firing (Fig. 1A). Using the RNAscope system for in situ mRNA detection (*27*), we examined the expression of mitochondria-encoded genes at the single-transcript level (fig. S1, A and B). We found that the mRNA of *Mtco1*, a mitochondria-encoded gene crucial for OXPHOS, was increased after PTX application (Fig. 1, A and D, and fig. S1C). This increase was prevented by a specific inhibitor of mitochondrial polymerase, IMT1B, that blocks mitochondrial DNA transcription (*28*), suggesting its dependence on transcription. To determine whether this process is also recruited by local synaptic stimuli, we infected excitatory neurons in the hippocampal CA3 region with an adeno-associated viral vector (AAV) carrying mCherry-tagged channelrhodopsin-2 (AAV2/9-P_{CaMKII}-hChR2^{H134R}-mCherry). To enable monosynaptic activation, we added the sodium channel blocker tetrodotoxin (TTX, 1 μM) to eliminate action potentials and the voltage-gated potassium channel blocker 4-aminopyridine (4-AP, 200 μM) to augment the light-induced depolarization. Photoactivation induced by 20-Hz, 470-nm blue light in the CA1 stratum radiatum (SR) region that receives projections from CA3 excitatory neurons increased *Mtco1* mRNA expression (Fig. 1B). This change was largely driven by postsynaptic activation in dendrites, as it was prevented in the presence of antagonists for *N*-methyl-D-aspartate receptors [NMDARs, 50 μM D-2-amino-5-phosphonovaleric acid (D-APV) and α-amino-3-hydroxy-5-methyl-4-isoxazolepropionic acid receptors (AMPARs, 10 μM 2,3-dioxo-6-nitro-7-sulfamoylbenzo[*f*]quinoxaline (NBQX)] (Fig. 1, B and D, and fig. S1C). Further, it was also inhibited by IMT1B, suggesting that mtDNA expression driven by synaptic activation occurs in a transcription-dependent manner.

To explore the in vivo recruitment of E-TC$_{mito}$, we activated hippocampal CA1 excitatory neurons (*27*), using a context-dependent foot shock protocol in mice. We found a transcription-dependent increase in *Mtco1* mRNA expression after the foot shock (Fig. 1, C and D, and fig. S1C). To further confirm these results, we conducted a quantitative real-time polymerase

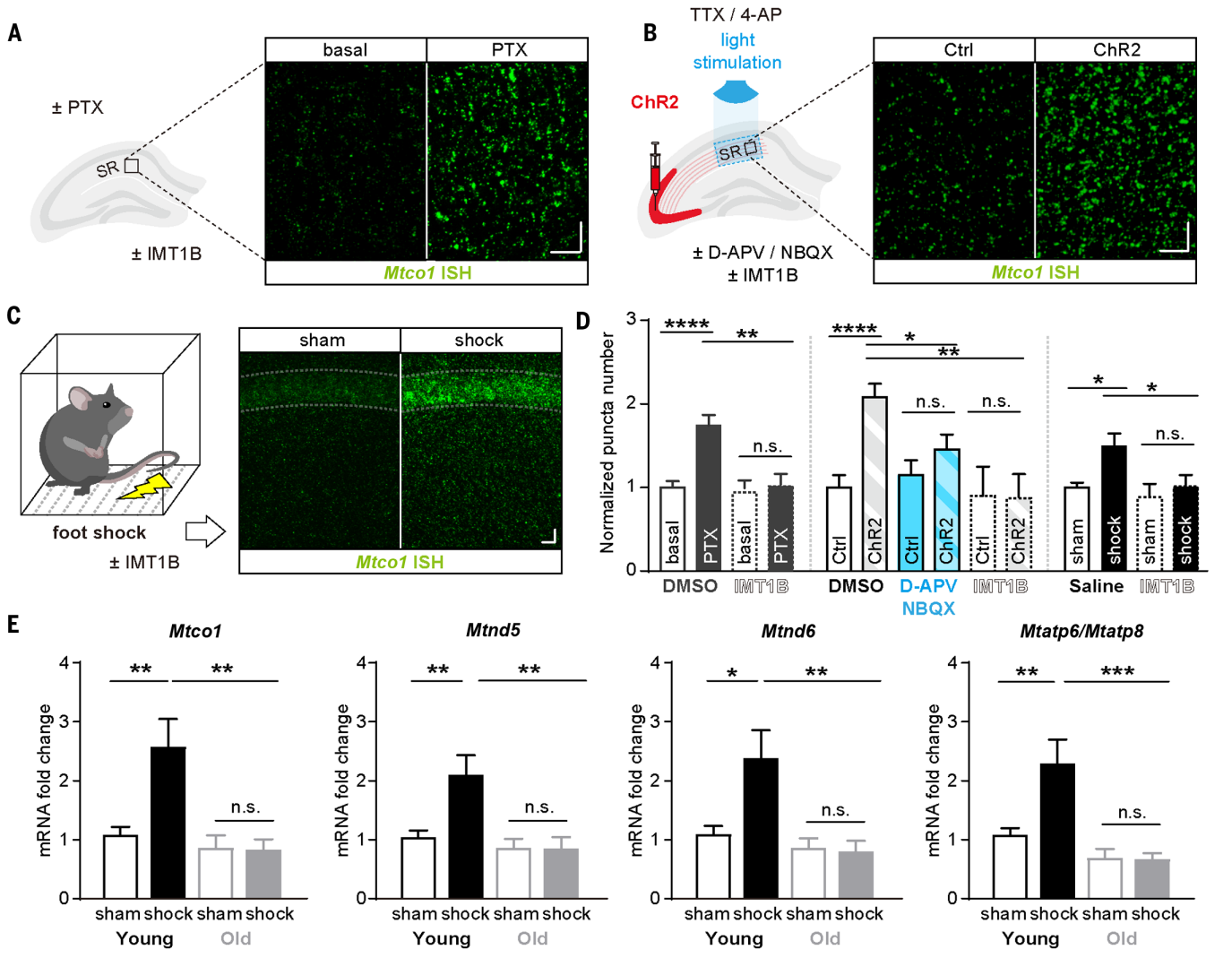

Fig. 1. Age-dependent mtDNA expression driven by neuronal and synaptic activity and experiences. (**A** to **D**) Representative images, alongside quantifications, depict in situ RNAscope analyses of *Mtco1* mRNA expression in acute hippocampal slices subjected to 50 μM PTX treatment for 1 hour [(A) and (D)] and exposed to 20-Hz blue light stimulation for 10 min [(B) and (D)] in the presence of 4-AP and TTX, and in mice sacrificed 1 hour after context-conditioned foot shocks [(C) and (D)] (N_{DMSO} = 21/12, N_{PTX} = 26/15, N_{IMT1B} = 14/8, $N_{IMT1b+PTX}$ = 10/8, N_{ctrl} = 22/12, N_{ChR2} = 23/12, $N_{D\text{-}APV+NBQX}$ = 11/8, $N_{D\text{-}APV+NBQX+ChR2}$ = 11/8, N_{IMT1B} = 5/2, $N_{IMT1B+ChR2}$ = 5/2, $N_{saline+sham}$ = 11/3, $N_{saline+shock}$ = 11/3, $N_{IMT1B+sham}$ = 11/3, $N_{IMT1B+shock}$ = 11/3 slices/animals). (**E**) Fold changes of mitochondrial transcripts, including *Mtco1*, *Mtnd5*, *Mtnd6*, *Mtatp6/Mtatp8*, were measured in the hippocampus of young mice (black) and 16-month-old mice (gray), with or without foot shocks (N_{young} = 13, N_{old} = 9 or 10 animals). In this and subsequent figures, summary data are presented as the mean ± SEM. One-way analysis of variance (ANOVA) followed by Tukey's test were used for all analysis in this figure. $^*P < 0.05$, $^{**}P < 0.01$, $^{***}P < 0.001$, $^{****}P < 0.0001$; n.s., not significant. Scale bar: 20 μm (A and C), 10 μm (B).

chain reaction (qRT-PCR) assay, using random hexamers and TaqMan probes to accommodate the substantial variability in length and polyadenylation in mitochondrial mRNAs (mt-mRNAs), allowing for a systematic analysis of the expression of mitochondria-encoded genes. Hippocampal mitochondria-encoded genes crucial for OXPHOS—including *Mtco1* (complex IV), *Mtnd5* (complex I, heavy chain), *Mtnd6* (complex I, light chain), and *Mtatp6/Mtatp8* (complex V)—increased their expression after the foot shock (Fig. 1E). However, nucleus-encoded mitochondrial genes such as *Sdha*, *Mtco4*, and *Atp5b* showed no changes (fig. S1, D to F). Additionally, both the mtDNA replication and transcription factor *Tfam* amount (fig. S1G) and the mtDNA copy number (fig. S1H) remained unaltered, indicating that E-TC_{mito}, recruited by experience, predominantly regulates mtDNA transcription, rather than replication.

Age-related decline in E-TC_{mito} and activity-dependent $[Ca^{2+}]_{mito}$

Given the substantial decline in synaptic function with aging (*29*–*31*), we examined the response of mitochondrial genes to neuronal activation by the context-shock pairing in aged mice. The increase in mtDNA expression in aged mice was diminished compared to the increase seen in young animals (Fig. 1E). Considering the pivotal role of calcium-dependent signaling in regulating DNA transcription and the link between neuronal excitation and activity-dependent mitochondrial calcium level ($[Ca^{2+}]_{mito}$) (*32*), we explored the possibility that the attenuated mtDNA expression increase in response to stimulation in aged mice could be related to changes in activity-dependent $[Ca^{2+}]_{mito}$. To investigate this hypothesis, we developed a green calcium sensor tagged with a mitochondrial targeting sequence (MTS) (*32*), which targets GCaMP6s to the mitochondrial matrix

(Mt-GCaMP6s) (fig. S2A). In primary neocortical neurons, expressing Mt-GCaMP6s did not affect the mitochondrial membrane potential (MMP) (fig. S2, B and C), and the specificity of this construct in detecting activity-dependent $[Ca^{2+}]_{mito}$ was validated using carbonyl cyanide 4-(trifluoromethoxy)phenylhydrazone (FCCP), a classic mitochondrial uncoupler that blocks mitochondrial calcium uptake (fig. S2D) (*33*). Driven by the Ca^{2+}-calmodulin–dependent protein kinase II alpha (αCaMKII) promoter to specifically target excitatory neurons, Mt-GCaMP6s was introduced into the primary somatosensory cortex of both young and aged mice via AAV. Mitochondrial calcium dynamics were then assessed in vivo using two-photon (2P) imaging 3 weeks after viral injection. Neuronal activation was achieved through whisker stimulation in awake, head-fixed mice. Activity-dependent $[Ca^{2+}]_{mito}$ was monitored in more than 2000 excitatory neurons, before and during stimulation, across all age groups (Fig. 2, A to C). In young mice, whisker stimulation led to an increase in $[Ca^{2+}]_{mito}$ (Fig. 2, A to C, and movie S1). However, in aged mice, this activity-dependent enhancement of $[Ca^{2+}]_{mito}$ was markedly attenuated (~3-fold less increase) (Fig. 2, D and E, and movie S2), indicating that experience-driven mitochondrial calcium influx declines with aging.

Activity-dependent $[Ca^{2+}]_{mito}$ is critical for E-TC_{mito}

Motivated by the identified association between diminished activity-dependent $[Ca^{2+}]_{mito}$ and mtDNA expression during aging, we examined the role of $[Ca^{2+}]_{mito}$ in E-TC_{mito} using primary neocortical neurons. To ascertain that E-TC_{mito} is regulated by neuronal activity, we incubated primary cultures with the $GABA_A$ receptor antagonist bicuculline (BIC, 40 μM, 1 hour) to enhance excitatory synaptic transmission and neuronal firing (*34*). This treatment not only increased $[Ca^{2+}]_{mito}$ (Fig. 2, F and G), but also enhanced mtDNA expression, including genes such as *Mtco1*, *Mtnd5*, *Mtnd6*, and *Mtatp6/Mtatp8* (Fig. 2H and fig. S2, E, H, I, and J), without altering the mtDNA copy number (fig. S2F) or their mRNA degradation (fig. S2G). The increase in mtDNA expression was transcription dependent, as it was prevented by IMT1B (fig. S2E). Additionally, it was inhibited (Fig. 2H and fig. S2, H to J) by blocking calcium channels with either the L-type voltage-gated calcium channel blocker nimodipine (Nim, 10 μM) or the NMDAR antagonist D-APV (50 μM), which prevented activity-dependent $[Ca^{2+}]_{mito}$ (Fig. 2, F and G). Furthermore, inhibiting activity-dependent $[Ca^{2+}]_{mito}$ with the intracellular Ca^{2+} chelator EGTA-AM (100 μM) (*33*), or by expressing the mitochondria-targeted calcium buffering protein parvalbumin (Mt-PV) (*35*) in excitatory neurons (Fig. 2, I and J, and fig. S2, K and L), abolished E-TC_{mito}, as evidenced by reduced activity-dependent mtDNA gene expression (Fig. 2K and fig. S2, M to O). Collectively, these findings suggest that E-TC_{mito} is reliant on activity-dependent $[Ca^{2+}]_{mito}$, setting it apart from E-TC_{nuc}, which can be activated in a nuclear Ca^{2+}-independent manner (*33*, *36*).

Activity-dependent regulation of $[Ca^{2+}]_{mito}$ and mtDNA expression by $CaMKII_{mito}$

If $[Ca^{2+}]_{mito}$ is pivotal in regulating E-TC_{mito}, how do mitochondria interpret neuronal activity to modulate their DNA expression? The mitochondrial calcium uniporter (MCU) plays a pivotal role in regulating mitochondrial calcium influx (*37*, *38*). Using the specific MCU inhibitor Ru360 (2 μM), we observed that activity-dependent $[Ca^{2+}]_{mito}$ was hindered in the absence of MCU opening (fig. S3A). Studies on cardiac muscle have implicated CaMKII in the regulation of MCU (*39*, *40*), a kinase known for decoding synaptic and neuronal activity through $Thr^{286/287}$ phosphorylation (pCaMKII) (*41*–*43*), and age-associated decline in activation (*44*, *45*). Coimmunoprecipitation assays revealed that αCaMKII, an isoform that is mainly expressed in excitatory neurons, forms a complex with calcium channels that orchestrate $[Ca^{2+}]_{mito}$ cascades, including ryanodine receptor 2 (RyR2), voltage-dependent anion channel 1 (VDAC1), and MCU (fig. S3B). Consistent with this, the CaMKII inhibitor KN93 (4 μM), but not its inactive congener KN92 (4 μM), prevented activity-dependent $[Ca^{2+}]_{mito}$, prompting inquiry into CaMKII's potential involvement in E-TC_{mito} (fig. S3, C and D).

Therefore, we conducted immunogold electron microscopy in the hippocampal SR region. Beyond the canonical distribution of αCaMKII in synapses, we identified its expression within neuronal mitochondria (fig. S3, E and F). To functionally explore the activation of mitochondrial CaMKII in response to neuronal activity, we treated neurons with BIC and then isolated the mitochondria to evaluate pCaMKII amounts within these organelles. Our findings demonstrated an increase in mitochondrial pCaMKII after stimulation (fig. S3, G and H). Having confirmed the presence and activity of CaMKII within neuronal mitochondria, we used CaMKIINtide, a peptide specifically inhibiting CaMKII (*46*), and targeted it to mitochondria (Mt-CaMKIINtide) (fig. S3I) to specifically modulate mitochondrial CaMKII functions (fig. S3J). In muscle cells, CaMKII in mitochondria senses calcium influx through MCU and phosphorylates sites such as Ser^{92} (S92) in its N-terminal domain located within the mitochondrial matrix. The phosphorylation site at S92 is highly conserved and plays an essential role in regulating calcium uptake through MCU (*39*, *47*, *48*). We found that the phosphorylation of S92 increased after BIC stimuli in neurons, which was prevented by Mt-CaMKIINtide (fig. S3, K and L). In line with these findings, introducing Mt-CaMKIINtide in excitatory neurons resulted in diminished $[Ca^{2+}]_{mito}$ in response to neuronal stimulation (Fig. 3, A and B). Concurrently, there was a reduction in the expression of mtDNA such as *Mtco1*, *Mtnd5*, *Mtnd6*, and *Mtatp6/Mtatp8* (Fig. 3C and fig. S3M), suggesting that Mt-CaMKII can phosphorylate MCU S92 in an activity-dependent manner, which in turn regulates $[Ca^{2+}]_{mito}$ and E-TC_{mito}.

Activity-dependent recruitment of $CREB_{mito}$ signaling in neurons

The results described above prompted us to investigate how mitochondria decode activity-dependent $[Ca^{2+}]_{mito}$ signals for their transcriptional regulation during aging. The D-loop, a crucial site governing both transcription and replication of mtDNA, has been suggested to harbor CRE-like sequences (*49*, *50*) that potentially interact with the transcription factor Ca^{2+}/cAMP response element–binding protein (CREB) (*51*, *52*). However, unlike the established role of CREB in E-TC_{nuc}, its existence and function in mitochondria have not been fully elucidated (*53*–*56*). Therefore, we conducted a DNA-affinity capture assay using multiple biotinylated DNA probes covering the major D-loop domain of neuronal mitochondria (Fig. 3D). The probe targeting the mtDNA noncoding region (nucleotides 15811 to 16050), which contains CRE-like sequences, interacted with mitochondrial CREB ($CREB_{mito}$), whose identity was confirmed through Western blot analysis using a specific CREB antibody (*57*). Furthermore, its subcellular distribution in neuronal mitochondria was affirmed through immunogold electron microscopy (Fig. 3E and fig. S4A).

To examine whether $CREB_{mito}$ is activated by synaptic and neuronal activity, we constructed a mitochondria-localized CREB activity sensor by fusing MTS with fluorescence resonance energy transfer (FRET) CREB activity biosensors (Mt-G-CREB, green; Mt-R-CREB, red) (*58*), which specifically respond to Ser^{133}-dependent activation of full-length CREB. At the basal state, overexpressed Mt-G-CREB colocalized with double-stranded DNA (fig. S4B), supporting the idea that CREB binds to mtDNA in neurons. In cultured hippocampal slices expressing Mt-R-CREB and Mt-GCaMP6s, we used 2P fluorescent lifetime imaging (2pFLIM) to simultaneously monitor the activation of $CREB_{mito}$ and $[Ca^{2+}]_{mito}$ (Fig. 3, F and G). We found that $CREB_{mito}$ was activated after the influx of $[Ca^{2+}]_{mito}$, which was evident from BIC-induced changes in Mt-R-CREB and Mt-GCaMP6s signals (Fig. 3, F and G). Furthermore, light-induced uncaging of Rubi-glutamate [median inhibitory concentration (IC_{50}) =7.7 μM] in proximity to dendrites triggered local changes in Mt-G-CREB FRET signals in dendrites of cultured neurons (Fig. 3, H and I). This response was prevented by FCCP or D-APV, suggesting that activity-dependent activation of mitochondrial CREB can be recruited by local synaptic stimuli

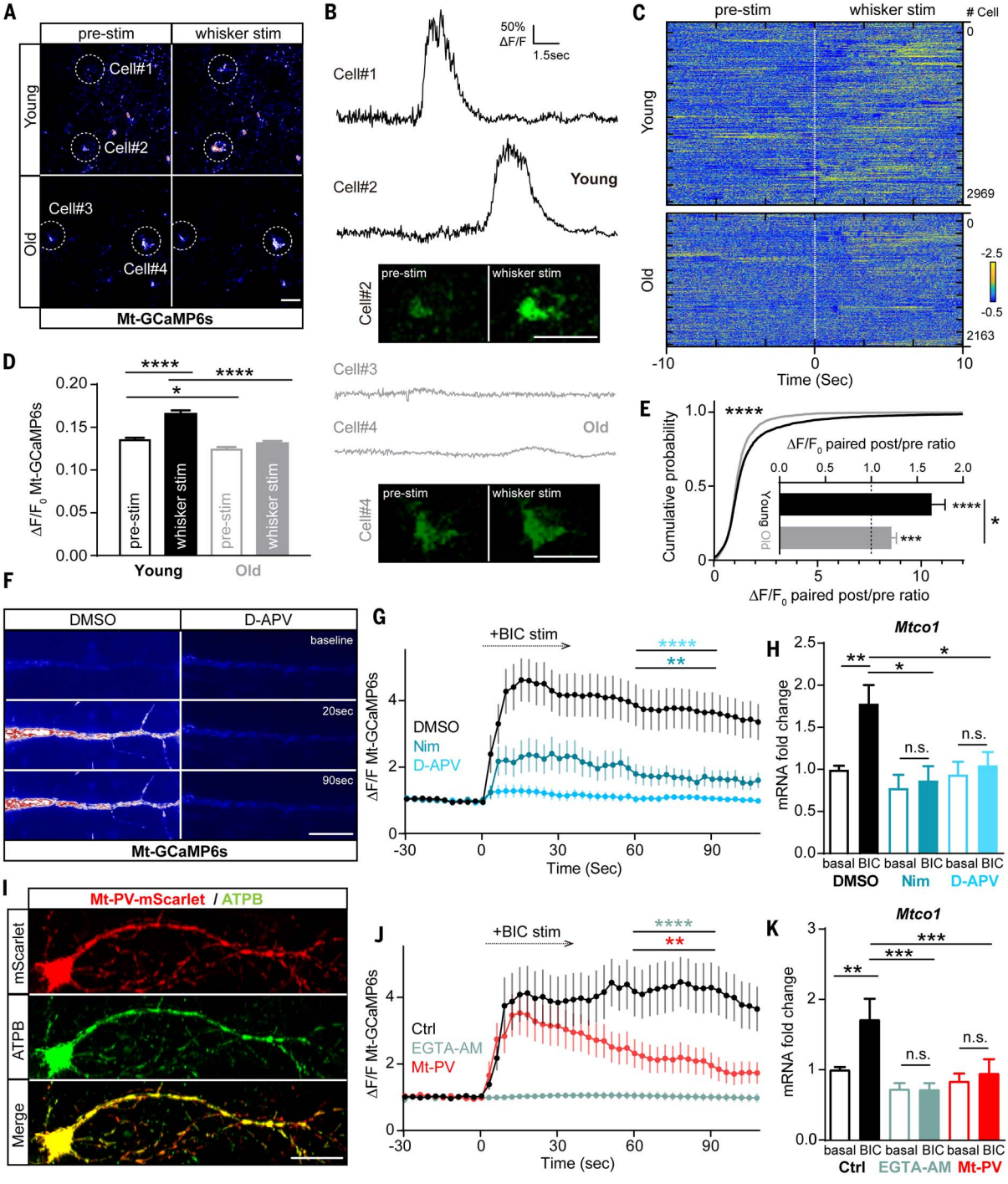

Fig. 2. Activity-dependent mitochondrial calcium influx in aging and its essential role in E-TC$_{mito.}$ (**A** to **E**) Representative in vivo images (A), traces (B), and heatmaps (C) for 2P imaging of Mt-GCaMP6s in L2/3 excitatory neurons in the somatosensory cortex from 3-month-old young (black) or 16-month-old aged (gray) male mice at basal states (for 10 s), or upon whisker stimulation (for 10 s), respectively. Quantification of Mt-GCaMP6s signal changes is shown in (D) and (E) (N_{young}= 2969/4, N_{old} = 2163/3 cells/animals). (**F** and **G**) Live imaging of primary neurons expressing BFP control and Mt-GCaMP6s after BIC application, preincubated with 0.05% dimethyl sulfoxide (DMSO) (black), 10 μM Nim (cerulean), or 50 μM D-APV (blue) for 10 min (*n* =10 to 14 cells). (**H**) Fold changes of mitochondrial transcript *Mtco1* amounts extracted from primary neurons after 1 hour of treatment with 40 μM BIC, treated with DMSO, Nim, or D-APV, were measured by qRT-PCR. (**I**) Representative image of primary neurons expressing Mt-PV-mScarlet, immunostained with a mouse antibody against ATP synthase F1 subunit beta (ATPB). (**J**) Same as (F) and (G) but loaded with 100 μM EGTA-AM (sage), or expressing Mt-PV (red) instead of control BFP in excitatory neurons (*n* = 10 to 13 neurons for each condition). (**K**) Similar to (H) but from neurons transduced with control BFP, loaded with DMSO, or EGTA-AM, and from neurons expressing Mt-PV-Scarlet (*n* = 9 to 18 wells for each condition). One-way ANOVA followed by Tukey's test for (D), (H), and (K); Kolmogorov-Smirnov test (cumulative distribution) for (E); two-tailed unpaired *t* test (bar graph) comparing young and old groups for (E); two-tailed paired *t* test (bar graph) analyzing ΔF/F0 paired post/pre ratio for (E); two-way ANOVA followed by Tukey's multiple comparison test for (G) and (J). *P < 0.05, **P < 0.01, ***P < 0.001, ****P < 0.0001; n.s., not significant. Scale bar: 20 μm.

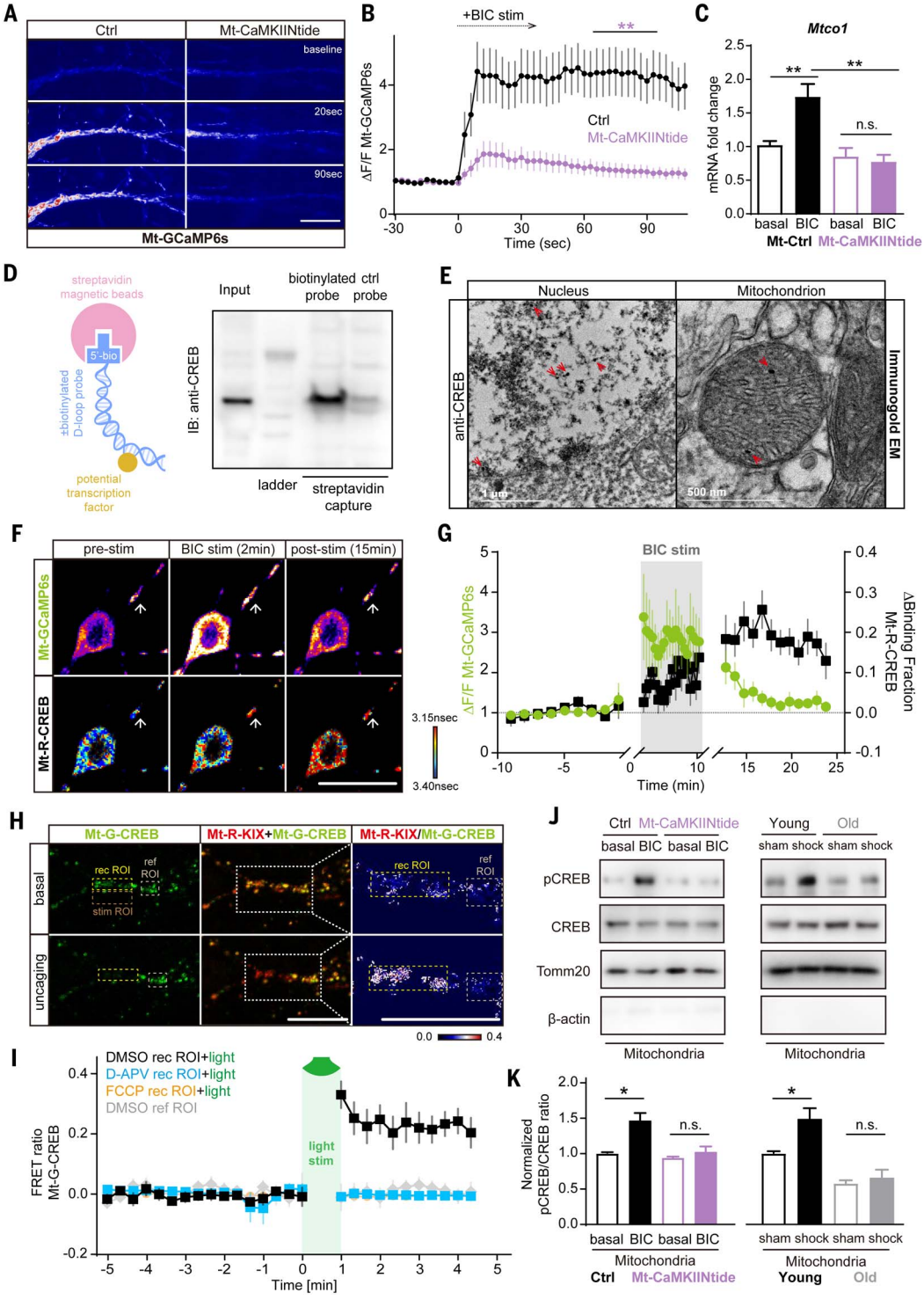

Fig. 3. CaMKII and CREB operate within neuronal mitochondria, mediating E-TC$_{mito}$ upon synaptic and neuronal activation. (**A** and **B**) Live imaging of primary neurons expressing control BFP (black) or Mt-CaMKIINtide (lilac), along with Mt-GCaMP6s, after BIC application (n = 10 to 18 cells for each condition). (**C**) Fold changes of mt-mRNA amounts extracted from primary neurons expressing BFP control or Mt-CaMKIINtide after 1 hour of BIC application (40 μM) measured by qRT-PCR (n = 9 to 12 neurons for each condition). (**D**) Schematic illustration of the DNA affinity capture assay. (**E**) Representative images of immunogold electron microscopy showing the subcellular localization of CREB in the rat hippocampal SR region. (**F** and **G**) Representative ex vivo images (F) depict 2pFLIM imaging of Mt-GCaMP6s (green) and Mt-R-CREB (red) in cultured hippocampal slices. BIC was perfused into the imaging system at time point 0 and washed out at the indicated time points. $\Delta F/F_0$ represents Mt-GCaMP6s response, and changes in Δbinding fraction of Mt-CREB sensors during stimulation are shown in (G) (N = 7 slices). (**H** and **I**) Representative images (H) and quantifications (I) of primary excitatory neurons expressing Mt-G-CREB subjected to 20-Hz, 470-nm light, which region-specifically uncaged 50 μM Rubi-Glu. Primary cultures were treated with DMSO (black), 50 μM D-APV (blue), or 5 μM FCCP (light orange). Stimulation, recording, and reference (gray) regions of interest (ROIs) were as indicated (n = 5 to 10 experiments for each condition). (**J** and **K**) Isolated mitochondrial fractions were obtained from primary neurons treated with BIC for 10 min. Fractions were also derived from the hippocampus of male mice sacrificed 1 hour after foot shock. Samples were subjected to immunoblot analysis using the indicated antibodies (n = 4 wells for primary culture experiments; n = 5 animals for in vivo experiments). Two-way ANOVA followed by Tukey's multiple comparison test for (B); one-way ANOVA followed by Tukey's test for (C) and (K); *P < 0.05, **P < 0.01; n.s., not significant. Scale bar: 1 μm (left) and 500 nm (right) for (E); 20 μm for (A), (F), and (H).

(Fig. 3, H and I). To monitor the activation of endogenous CREB$_{mito}$, we used a specific antibody against phosphorylated CREB at Ser^{133} (pCREB) (fig. S4, C and D, see legends). Consistent with CREB activity sensor results, we found an increase in mitochondrial pCREB (pCREB$_{mito}$) after BIC stimuli (Fig. 3, J and K). Unlike non-mitochondrial pCREB or nuclear pCREB, the activity-induced increase in pCREB$_{mito}$ was specifically prevented by Mt-CaMKIINtide (Fig. 3, J and K, left panel; fig. S4, E to H). Moreover, this dynamic change diminished in aged brains: Context-conditioned foot shocks induced substantial pCREB$_{mito}$ in the hippocampus of young adult mice, a response that was absent in old mice (Fig. 3, J and K, right panel).

The critical role of E-TC$_{mito}$ in regulating synaptic and mitochondrial resilience amid activity changes

To elucidate the role of CREB$_{mito}$ in regulating E-TC$_{mito}$ and neuronal function, we created

Mt-A-CREB (fig. S5A) by combining MTS with the CREB inhibitory peptide, A-CREB (*59*). Overexpression of Mt-A-CREB in neuronal mitochondria impeded the BIC-induced expression of mtDNA, including *Mtco1*, *Mtnd5*, *Mtnd6*, and *Mtatp6/Mtatp8* (Fig. 4A and fig. S5, B to D). By contrast, the activity-dependent expression of $CREB_{nuc}$ target genes, such as c-*fos* and *Arc*, remained unaffected (fig. S5, E and F), suggesting that Mt-A-CREB specifically influences E-TC_{mito}. We then delivered an AAV expressing Mt-A-CREB or its control Mt-mNeonGreen to the mature cortex through bilateral stereotactic injection (fig. S6A). Whole-cell recordings revealed that expressing Mt-A-CREB in excitatory neurons in layer 2/3 of the primary somatosensory cortex did not affect the resting membrane potential (fig. S6B) and the input-output function measured from the number of action potentials evoked by delivering current pulses of incremental intensity (fig. S6, C and D). Additionally, we observed no differences in the paired-pulse ratio at various interpulse intervals (fig. S6, E and F) and the frequency of spontaneous excitatory postsynaptic currents (sEPSCs) (fig. S6G), indicating largely consistent presynaptic functions. However, we found that the amplitude of sEPSCs in excitatory neurons expressing Mt-A-CREB was reduced compared to that in neurons expressing the control Mt-mNeonGreen (Fig. 4, B and C), suggesting that basal AMPAR-mediated excitatory postsynaptic transmission, which is spared in the absence of E-TC_{nuc} (*60*), is particularly vulnerable to disrupted E-TC_{mito}. To further validate these findings and to understand the molecular mechanisms responsible for the decreased amplitude of sEPSC, we quantified the surface expression of AMPAR GluA1 subunits (sGluA1) in cultured neurons (Fig. 4, D and E). Consistent with our findings in slices, we found a reduction in the basal amounts of sGluA1, with total GluA1 remaining unaffected in the presence of Mt-A-CREB (fig. S6H).

To understand the role of E-TC_{mito} in synaptic strength regulation, we explored the relationship between neuronal activity and sGluA1 amounts in the presence or absence of Mt-A-CREB. We used NLS-mScarlet, a nuclear-localized red fluorescent protein activated by the robust activity marking (RAM) promoter (*61*), and coexpressed it with mNeonGreen, driven by an activity-independent promoter, in a unified construct. The red (NLS-mScarlet) to green (mNeonGreen) fluorescence ratio, which correlates positively with the occurrence of neuronal activity, allowed us to track the activity experiences of neurons (fig. S6, I to L). We found a negative correlation between sGluA1 amounts and NLS-mScarlet intensity in neurons expressing Mt-A-CREB (fig. S6M), unlike in neurons with Mt-mNeonGreen (fig. S6N). This indicates that E-TC_{mito} disruption may impair neurons' ability to sustain sGluA1 expression amid increased neuronal activity, potentially affecting the homeostatic regulation of synaptic strength such as synaptic scaling. To examine this hypothesis, we exposed cultured neurons to 24 hours of BIC treatment to induce classic synaptic down-scaling (*34*), followed by assessing synaptic recovery after BIC removal (Fig. 4, F and G). In neurons with Mt-A-CREB, we found more rapid synaptic down-scaling (Fig. 4F) and slower recovery (Fig. 4G). Even 72 hours after BIC withdrawal, sGluA1 amounts in neurons expressing Mt-A-CREB had not reverted to baseline, whereas in control neurons expressing Mt-mNeonGreen, full recovery was achieved within 24 hours (Fig. 4G). Collectively, these findings suggest that the absence of E-TC_{mito} compromises synaptic homeostasis, leading to diminished synaptic resilience in response to activity changes.

Given that postsynaptic transmission is largely fueled by mitochondria (*15*, *62*–*64*), we asked whether disrupted synaptic resilience is linked to impaired energy supply in the absence of E-TC_{mito}. To test this, we measured the intracellular ATP reserve in cultured neurons and found that the ATP amount in neurons expressing Mt-A-CREB was significantly lower compared to that in neurons expressing the control Mt-mTagBFP2 (Fig. 4H). To further investigate whether the synaptic ATP pool is affected in the absence of E-TC_{mito}, we designed a postsynaptic ATP sensor, namely PSD95 FingR-MalionG-mCherry (Fig. 4, I and J, upper panel). This sensor was created by combining the ATP sensor MalionG (*65*) with fibronectin intrabodies generated through mRNA display (FingRs) (*66*), specifically targeting the endogenous postsynaptic density protein PSD95 (fig. S6O). The ratio of green/red fluorescence, emitted by MalionG and mCherry respectively, highlighted a lower postsynaptic ATP reserve in neurons expressing Mt-mTagBFP2-A-CREB (Fig. 4, I and J). To examine whether an energy deficit in the absence of E-TC_{mito} could play a role in synaptic weakening, we overexpressed the cytosolic brain-type creatine kinase (CK-B), which is known to regenerate ATP via the phosphocreatine system independently of mitochondria (*15*, *67*, *68*). We observed that CK-B increased sGluA1 amounts (fig. S6, P and Q). The difference in sGluA1 due to the presence of Mt-A-CREB almost disappeared in neurons expressing CK-B (fig. S6, P and Q), supporting the notion that decreased ATP might play an important role in synaptic weakening in Mt-A-CREB neurons.

To explore potential mechanisms underlying decreased ATP reserves in neurons, we examined whether impairment of E-TC_{mito} affects mitochondrial proteins and performance. As demonstrated by both Western blot analysis and immunostaining, mtDNA-encoded protein expression was increased after BIC stimuli (fig. S7, A to C). This activity-dependent change occurs throughout the neuron, with *Mtco1* expression rising in both the soma and dendrites (fig. S7, C and D), a process inhibited by Nim, D-APV (fig. S7, C to E), IMT1B (fig. S7, F and G), and Mt-CaMKIINtide (fig. S7, H and I). Although the mRNA amounts of the nucleus-encoded OXPHOS gene *Mtco4* did not change after the stimulation (fig. S1D), we observed that the Mtco4 protein expression in mitochondria increased with BIC stimuli, a phenomenon curtailed by Mt-CaMKIINtide (fig. S4D). This aligns with prior research demonstrating that the expression of mitochondria-encoded OXPHOS genes serves as a gatekeeper (*69*), regulating the translation of nucleus-encoded mitochondrial genes—a process influenced by neuronal activity (*22*). To further scrutinize the role of E-TC_{mito} in regulating the mtDNA-encoded mitochondrial protein, we implemented several approaches: Ru360 application to inhibit mitochondrial calcium uptake (fig. S7, J and K), Mt-PV overexpression to block activity-dependent $[Ca^{2+}]_{mito}$ (fig. S7, L and M), and Mt-A-CREB overexpression to inhibit $CREB_{mito}$ activation (fig. S7N). Compared with their respective controls, these manipulations prevented the activity-induced increase in Mtco1, reinforcing the notion that E-TC_{mito} likely play a critical role in the activity-dependent control of mitochondrial proteins in neurons. Moreover, this activity-dependent process carries functional relevance in regulating MMP, which is essential for ATP production (*70*, *71*). Our results revealed that basal MMP was lower in neurons expressing Mt-A-CREB (Fig. 4, K and L), consistent with lower ATP amounts in neurons with $CREB_{mito}$ activation blocked (Fig. 4, H to J). Furthermore, the dynamic change of MMP after neuronal activity was also affected. Compared with neurons that expressing the control Mt-mNeonGreen, neurons expressing Mt-A-CREB exhibited a slower recovery of MMP after stimulation (Fig. 4M). In concert, these findings suggest that E-TC_{mito} establishes an activity-dependent control over mitochondrial resilience, influencing various aspects of mitochondria that are known to deteriorate with aging (*72*).

E-TC_{mito} in vivo and its potential to revitalize functions in the aged brain

We also asked whether E-TC_{mito} could contribute to experience-dependent mtDNA expression in vivo, and if so, how it is linked to impairments in aged brains. We generated knock-in pCAG-loxp-STOP cassette-loxp-Mt-mNeonGreen-A-CREB transgenic mice (fig. S8A). By selectively inhibiting CREB in the mitochondria of excitatory neurons through crossbreeding with vGluT2-Cre mice (hereafter referred to as Mt-A-CREB mice, Fig. 5A and fig. S8B), we examined the cognitive impact of inhibiting $CREB_{mito}$ in vivo. Behavioral assessments showed that Mt-A-CREB mice exhibited normal functions in the forced-swim test for depressive-like behaviors, the open field and elevated plus maze tests for anxiety and

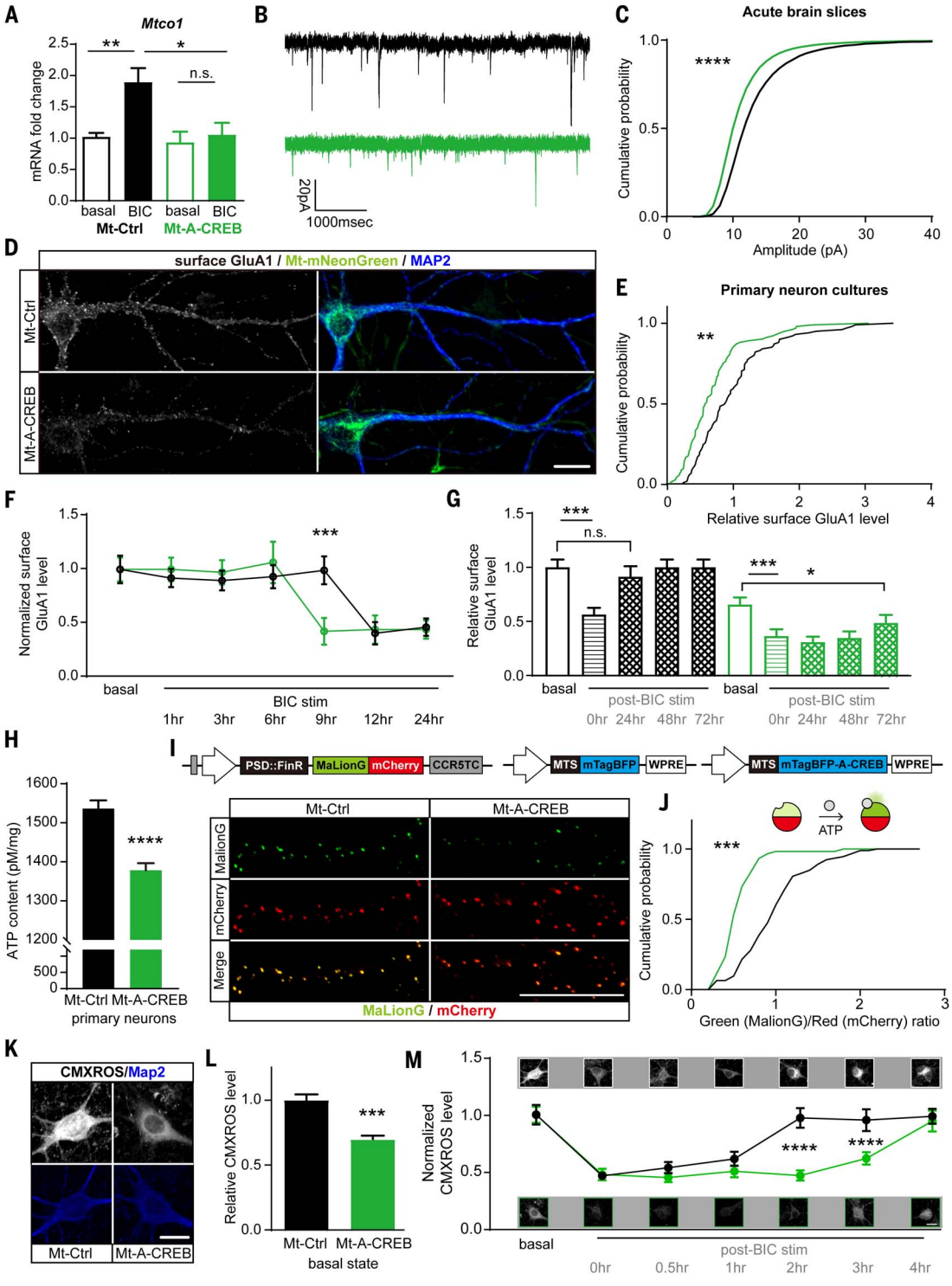

Fig. 4. E-TC$_{mito}$ regulates mitochondrial and synaptic resilience amidst activity changes. (**A**) Fold changes of mt-mRNA amounts extracted from primary neurons expressing Mt-mNeonGreen (referred as Mt-Ctrl, black) or Mt-mNeonGreen-A-CREB (green) after 1 hour of BIC application (n = 10 to 15 for each condition). (**B** and **C**) Representative sEPSC traces (B) and quantification (C) of whole-cell voltage-clamp recordings from L2/3 pyramidal neurons in acute coronal cortical slices expressing Mt-Ctrl (black) or Mt-A-CREB (green) from male mice aged 6 to 8 weeks ($N_{Mt\text{-}Ctrl}$ = 15/5, $N_{Mt\text{-}A\text{-}CREB}$ = 16/5, cells/animals). (**D** and **E**) Representative images (D) and quantifications (E) of surface GluA1 staining in primary neurons expressing Mt-Ctrl or Mt-A-CREB in the unstimulated state during days in vitro 14 to 18 (N = 3 cultures, n > 100 cells for each condition). (**F** and **G**) Relative sGluA1 intensity in primary neurons expressing Mt-Ctrl or Mt-A-CREB with the indicated BIC treatment (normalized to their respective basal conditions) (F), or (G) at the indicated times after the withdrawal of 24-hour BIC stimulation (N = 2 cultures, n > 50 cells for each condition, normalized to Mt-Ctrl at basal conditions). (**H**) Luciferase-based analysis of ATP content in primary cultured neurons expressing Mt-Ctrl (black) or Mt-A-CREB (green) (n = 8 to 12 wells). (**I** and **J**) Schematic illustration of the structure of synaptic ATP sensor. Representative images (I) and quantifications (J) of neurons expressing Mt-mTagBFP2 or Mt-mTagBFP2-A-CREB (N = 2 cultures). (**K** to **M**) Representative images (K) and quantifications of neurons expressing Mt-Ctrl or Mt-A-CREB, stained with 50 nM CMXROS for 15 min before fixation. Relative CMXROS intensity (normalized to Mt-Ctrl) (L), and after stimulation with BIC for 1 hour, as well as at 0.5, 1, 2, 3, or 4 hours after BIC treatment (M) (N = 5 cultures, n = ~70 to 120 cells for each condition, normalized to their respective basal conditions). Kolmogorov-Smirnov test for (C) and (E) (cumulative distribution); one-way ANOVA followed by Tukey's test for (A) and (G); two-way ANOVA followed by Tukey's multiple comparison test for (F) and (M); unpaired t test for the rest. *P < 0.05, **P < 0.01, ***P < 0.001, ****P < 0.0001; n.s., not significant. Scale bar: 20 μm.

motor functions, and the three-chamber test for sociability (fig. S8, C to G). However, a cognitive deficit was observed in the novel location recognition test after a 2-hour retention interval (Fig. 5B and fig. S8H), whereas performance remained consistent in the 15-min retention scenario (fig. S8, I and J) and the Y maze test (fig. S8, K and L). Further investigation of memory performance using the contextual fear conditioning (CFC) task revealed that Mt-A-CREB mice exhibited reduced freezing behavior after a 24-hour retention period (Fig. 5C). Thus, both hippocampus-dependent spatial memory and fear memory, as indicated by performance in the novel location recognition

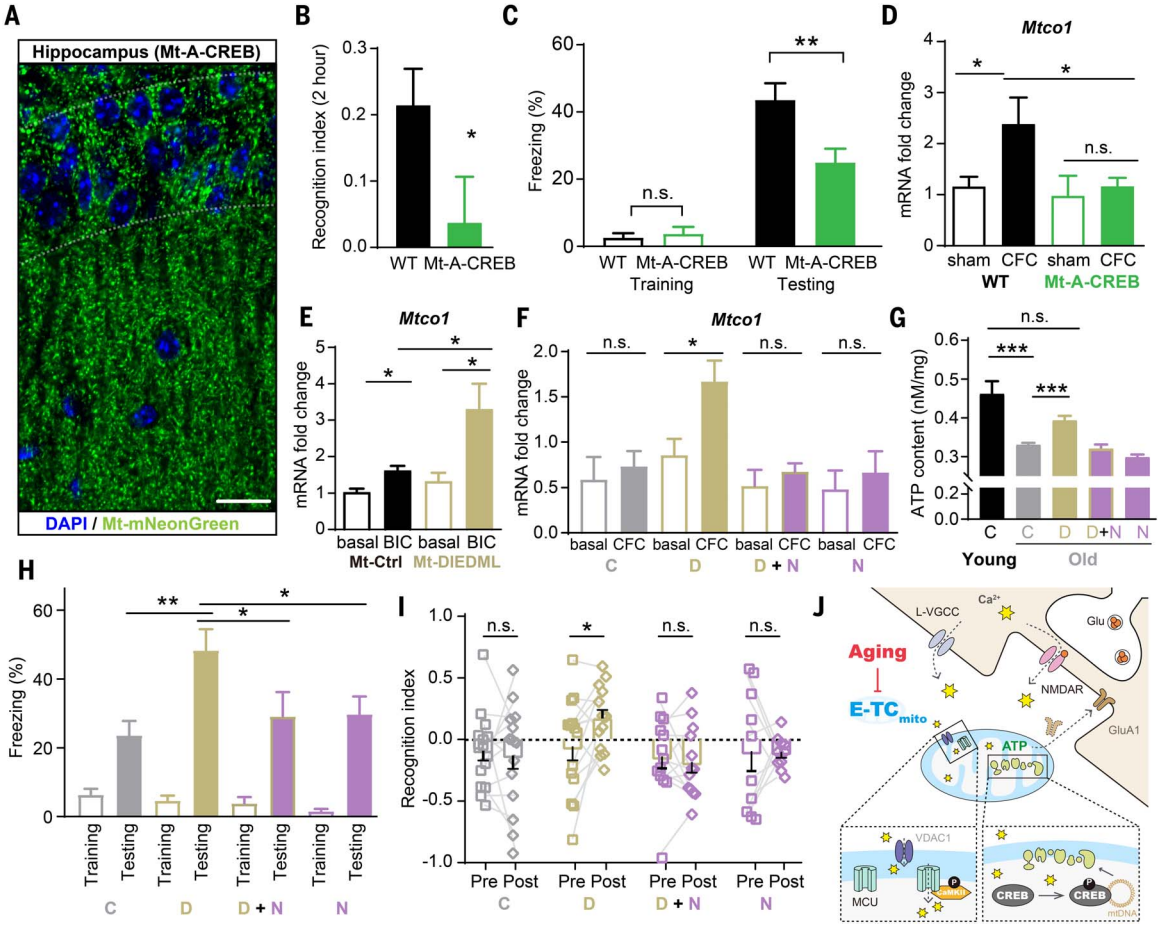

Fig. 5. The in vivo role of E-TC$_{mito}$ and its potential to revitalize functions in the aged brain. (**A**) Representative image of the hippocampal CA1 region of Mt-A-CREB mice. (**B**) Recognition index of Mt-A-CREB mice (green) and wild-type (WT) littermates (black) after a 2-hour retention interval in a novel location test (N_{WT} = 20, $N_{Mt\text{-}A\text{-}CREB}$ = 14 animals). (**C**) Freezing behavior percentages of Mt-A-CREB and WT littermates 24 hours after foot shock in a CFC test (N_{WT} = 21, $N_{Mt\text{-}A\text{-}CREB}$ = 21 animals). (**D**) Fold changes of mitochondrial transcripts extracted from hippocampus of young WT or MT-A-CREB mice with or without CFC (N_{WT} = 11 to 13, $N_{Mt\text{-}A\text{-}CREB}$ = 5 to 11 animals). (**E**) Fold changes of mt-mRNA amounts extracted from primary neurons expressing Mt-mNeonGreen (referred as Mt-Ctrl, black) or Mt-mNeonGreen-CREB^{DIEDML} (olive brown) after a 1-hour BIC application (n = 9 to 11 wells for each condition). (**F**) Fold changes of mitochondrial transcripts extracted from the hippocampus of aged mice infected with indicated viruses with or without CFC. The viruses included Mt-mNeonGreen (Mt-Ctrl, gray), Mt-CREB^{DIEDML} (olive brown), a mixture of Mt-CREB^{DIEDML}+Mt-CaMKIINtide (olive brown + lilac), and Mt-CaMKIINtide (lilac) ($N_{Mt\text{-}ctrl}$ = 6 to 8, $N_{Mt\text{-}CREB\ DIEDML}$ = 5 to 7, N_{D+N} = 4 to 6, $N_{Mt\text{-}CaMKIINtide}$ = 4 to 6 animals). (**G**) Hippocampal ATP was extracted and measured using bioluminescence in 3-month-old young mice (black) and 18-month-old mice as indicated (N = 9 wells and 3 animals for each condition). (**H**) Eighteen-month-old mice were tested in a CFC test 24 hours after CFC ($N_{Mt\text{-}ctrl}$ = 10, $N_{Mt\text{-}CREB\ DIEDML}$ = 8, N_{D+N} = 9, $N_{Mt\text{-}CaMKIINtide}$ = 9 animals). (**I**) Eighteen-month-old mice were examined in a novel location test after a 2-hour retention interval ($N_{Mt\text{-}ctrl}$ = 15, $N_{Mt\text{-}CREB\ DIEDML}$ = 14, N_{D+N} = 13, $N_{Mt\text{-}CaMKIINtide}$ = 10 animals). (**J**) Schematic illustration of E-TC$_{mito}$. Two-tailed unpaired t test for (B), (C), and (F); one-way ANOVA followed by Tukey's test for (D), (E), (G), and (H); two-tailed paired t test for (I); $^*P < 0.05$, $^{**}P < 0.01$, $^{***}P < 0.001$, n.s., not significant. Scale bar: 20 μm.

test and the CFC task, respectively, were disrupted in Mt-A-CREB mice. Additionally, and in alignment with the critical role of CREB$_{mito}$ in E-TC$_{mito}$, a complete absence of CFC-induced mtDNA expression of genes such as *Mtco1*, *Mtnd5*, *Mtnd6*, and *Mtatp6/Mtatp8* was noted in Mt-A-CREB mice (Fig. 5D and fig. S8, M to O).

Given the identified main role of E-TC$_{mito}$ and its association with aging, we next investigated the potential of manipulating CREB$_{mito}$ to counteract age-related brain function deterioration. We engineered Mt-CREB^{DIEDML} by fusing MTS with a constitutively active CREB variant, CREB^{DIEDML} (fig. S9A) (*73*, *74*). This variant moderately increases CREB-mediated transcription under basal conditions (*74*) and achieves its maximum effect in inducing CREB-gene expression with activity-dependent calcium increase in neurons (*74*, *75*). Expressing Mt-CREB^{DIEDML} in cultured neurons boosted mtDNA expression (Fig. 5E and fig. S9, B to D) after BIC stimuli. Additionally, it increased the amounts of ATP (fig. S9E) and sGluA1 (fig. S9, F and G), while sparing MMP under basal conditions (fig. S9H). Moreover, Mt-CREB^{DIEDML} accelerated the recovery of both MMP (fig. S9I) and sGluA1 (fig. S9G) after BIC stimuli, confirming that Mt-CREB^{DIEDML} plays a dominant active role in regulating mitochondrial and synaptic performance. Leveraging this functional advantage, we bilaterally delivered an AAV expressing the gene encoding Mt-CREB^{DIEDML} into the hippocampus of 16-month-old mice (fig. S9J) and assessed hippocampus-dependent memory performance. In the CFC task, mtDNA expression induced by experience was enhanced in aged mice expressing Mt-CREB^{DIEDML} (Fig. 5F and fig. S9, J and K). Furthermore, brain ATP reserves were restored in the presence of Mt-CREB^{DIEDML} (Fig. 5G), increasing the ATP amount in the hippocampus of aged mice to amounts comparable to that in young mice. Behaviorally, aged mice

expressing Mt-CREB^{DIEDML} displayed enhanced memory in the CFC task (Fig. 5H and fig. S9, L and M). Furthermore, in the novel location recognition test—a measure in which performance deteriorates with age (fig. S9, N and O)—individual mice showed substantial memory improvements 2 months after Mt-CREB^{DIEDML} expression compared to their respective performance baseline before expression (Fig. 5I and fig. S9P). This longitudinal analysis highlights the effectiveness of Mt-CREB^{DIEDML} in mitigating age-related memory deficits within the same subjects over time. The beneficial effects of Mt-CREB^{DIEDML}, encompassing aspects such as neuronal ATP reserves and memory performance, were abolished with the coexpression of Mt-CaMKIINtide. Taken together, these findings suggest that E-TC$_{mito}$ is not only essential for maintaining brain function through use-dependent mechanisms but might also offer a potential target for mitigating age-related decline (Fig. 5J).

Discussion

Here, we examined the dynamic interplay among neuronal mitochondrial mass (mtDNA expression), bioenergetic demands (ATP reserves), and information processing (synaptic transmission and memory) in the brain and with aging. Our study uncovered key molecular cascades underlying activity-dependent mtDNA transcription and the important role of this process in sustaining mitochondrial performance in an experience-driven manner. This enables feedback control on neuronal energy reserves to support synaptic and mnemonic functions, providing a molecular framework for understanding how enhancing mental activity could counteract cognitive aging (*76*, *77*).

Mitochondria are crucial in supporting major brain functions, ranging from energy production (*12*, *14*, *15*) and calcium buffering (*78*), to synaptic transmission (*13*, *79*, *80*), long-term synaptic plasticity (*15*, *62*, *81*, *82*), neuronal firing (*83*–*85*), and memory (*86*–*88*). In this context, exploring the molecular mechanisms of E-TC$_{mito}$ offers a valuable opportunity to investigate the intricate interplay among these mitochondrial functions within the brain, particularly in an activity-dependent manner. A question of particular interest is whether the decreased synaptic strength observed in the absence of E-TC$_{mito}$, is indicative of mitochondria-mediated alterations in the neuronal firing set point (*84*). Furthermore, unraveling how E-TC$_{mito}$, especially its role in regulating activity-dependent energy adaptations, is linked to synaptic anchoring (*89*), neuronal calcium dynamics, and long-term synaptic plasticity (*29*, *30*) presents an exciting area for future research. A recent study suggests that ~80 to 90% of axonal mitochondria in cortical pyramidal neurons could be devoid of mtDNA (*90*), indicating that mitochondrial regulation may be distinct between axon and dendrites. This might explain why we found a more pronounced impact of mitochondrial CREB on postsynaptic functions as opposed to presynaptic ones. Nevertheless, in young brains, a balance between energy reserves, synaptic function, and mtDNA expression forms a dynamic regulatory network essential for processing and encoding information. However, with aging, this delicately balanced system undergoes profound changes. Synaptic functions diminish, paralleled by a decline in mitochondrial conditions and capacities, marking the aging process's cumulative impact on the brain's energetic ecosystem (*72*). By exploring the molecular mediators of E-TC$_{mito}$, our research contributed to elucidate these complex regulatory mechanisms. It suggests that experience-driven mtDNA expression is attenuated because of either diminished activity input or impaired E-TC$_{mito}$ function during the aging process. One of the most promising implications of our research is its potential for therapeutic intervention in age-related cognitive decline. By engineering a dominant active form of CREB$_{mito}$, we demonstrated the potential to enhance activity-dependent mtDNA expression in aged mammalian brains, effectively replenishing neuronal energy reserves and improving memory functions. Thus, enhancing E–TC$_{mito}$ might represent a valuable strategy to counteract the decline in brain functions associated with aging.

Summary of materials and methods

All animal experiments were approved by the Animal Care and Use Committee at Zhejiang University and were conducted in accordance with institutional guidelines regarding the care and use of laboratory animals. Constructs generated in this project were confirmed using Sanger sequencing. Experiments related to primary neurons were largely performed as previously described (*36*). Where indicated, drugs were added before and included throughout the stimulation unless otherwise specified. qRT-PCR was performed as previously reported with minor adjustments (*57*). Mitochondrial mRNA levels were assessed using commercial TaqMan probe primer sets from Accurate Biology Probe Database, amplified by Pro-Taq HS. Nuclear mRNA levels were assessed using SYBR Green, and specific primers targeting mouse genes were purchased from Origene. 2pFLIM experiments with organotypic mouse hippocampal slice cultures were performed as described previously (*58*). Electrophysiology and most behavioral tests were carried out as previously reported with minor adjustments (*27*). All summary data are expressed as the mean ± SEM. Statistical analyses were performed using Prism (GraphPad Software). For more a detailed explanation of experimental procedures and analysis, see the supplementary materials and methods.

REFERENCES AND NOTES

1. M. Ximerakis *et al*., Single-cell transcriptomic profiling of the aging mouse brain. *Nat. Neurosci.* **22**, 1696–1708 (2019). doi: 10.1038/s41593-019-0491-3; pmid: 31551601
2. I. G. Onyango *et al*., Regulation of neuron mitochondrial biogenesis and relevance to brain health. *Biochim. Biophys. Acta* **1802**, 228–234 (2010). doi: 10.1016/j.bbadis.2009.07.014; pmid: 19682571
3. J. I. Morgan, T. Curran, Role of ion flux in the control of c-fos expression. *Nature* **322**, 552–555 (1986). doi: 10.1038/322552a0; pmid: 2426600
4. M. E. Greenberg, E. B. Ziff, L. A. Greene, Stimulation of neuronal acetylcholine receptors induces rapid gene transcription. *Science* **234**, 80–83 (1986). doi: 10.1126/science.3749894; pmid: 3749894
5. A. E. West, E. C. Griffith, M. E. Greenberg, Regulation of transcription factors by neuronal activity. *Nat. Rev. Neurosci.* **3**, 921–931 (2002). doi: 10.1038/nrn987; pmid: 12461549
6. J. P. Adams, S. M. Dudek, Late-phase long-term potentiation: Getting to the nucleus. *Nat. Rev. Neurosci.* **6**, 737–743 (2005). doi: 10.1038/nrn1749; pmid: 16136174
7. K. Deisseroth, P. G. Mermelstein, H. Xia, R. W. Tsien, Signaling from synapse to nucleus: The logic behind the mechanisms. *Curr. Opin. Neurobiol.* **13**, 354–365 (2003). doi: 10.1016/S0959-4388(03)00076-X; pmid: 12850221
8. H. Bading, Nuclear calcium signalling in the regulation of brain function. *Nat. Rev. Neurosci.* **14**, 593–608 (2013). doi: 10.1038/nrn3531; pmid: 23942469
9. U. Frey, R. G. Morris, Synaptic tagging and long-term potentiation. *Nature* **385**, 533–536 (1997). doi: 10.1038/385533a0; pmid: 9020359
10. C. M. Alberini, E. R. Kandel, The regulation of transcription in memory consolidation. *Cold Spring Harb. Perspect. Biol.* **7**, a021741 (2014). doi: 10.1101/cshperspect.a021741; pmid: 25475090
11. H. Ma *et al*., Excitation-transcription coupling, neuronal gene expression and synaptic plasticity. *Nat. Rev. Neurosci.* **24**, 672–692 (2023). doi: 10.1038/s41583-023-00742-5; pmid: 37773070
12. S. Li, Z. H. Sheng, Energy matters: Presynaptic metabolism and the maintenance of synaptic transmission. *Nat. Rev. Neurosci.* **23**, 4–22 (2022). doi: 10.1038/s41583-021-00535-8; pmid: 34782781
13. M. J. Devine, J. T. Kittler, Mitochondria at the neuronal presynapse in health and disease. *Nat. Rev. Neurosci.* **19**, 63–80 (2018). doi: 10.1038/nrn.2017.170; pmid: 29348666
14. C. N. Hall, M. C. Klein-Flügge, C. Howarth, D. Attwell, Oxidative phosphorylation, not glycolysis, powers presynaptic and postsynaptic mechanisms underlying brain information processing. *J. Neurosci.* **32**, 8940–8951 (2012). doi: 10.1523/JNEUROSCI.0026-12.2012; pmid: 22745494
15. V. Rangaraju, M. Lauterbach, E. M. Schuman, Spatially Stable Mitochondrial Compartments Fuel Local Translation during Plasticity. *Cell* **176**, 73–84.e15 (2019). doi: 10.1016/j.cell.2018.12.013; pmid: 30612742
16. M. B. Hock, A. Kralli, Transcriptional control of mitochondrial biogenesis and function. *Annu. Rev. Physiol.* **71**, 177–203 (2009). doi: 10.1146/annurev.physiol.010908.163119; pmid: 19575678
17. J. M. Williams, V. L. Thompson, S. E. Mason-Parker, W. C. Abraham, W. P. Tate, Synaptic activity-dependent modulation of mitochondrial gene expression in the rat hippocampus. *Brain Res. Mol. Brain Res.* **60**, 50–56 (1998). doi: 10.1016/S0169-328X(98)00165-X; pmid: 9748499
18. R. M. Cowell, K. R. Blake, J. W. Russell, Localization of the transcriptional coactivator PGC-1alpha to GABAergic neurons during maturation of the rat brain. *J. Comp. Neurol.* **502**, 1–18 (2007). doi: 10.1002/cne.21211; pmid: 17335037
19. M. J. Kennedy, M. D. Ehlers, Organelles and trafficking machinery for postsynaptic plasticity. *Annu. Rev. Neurosci.* **29**, 325–362 (2006). doi: 10.1146/annurev.neuro.29.051605.112808; pmid: 16776589
20. V. Rangaraju, S. Tom Dieck, E. M. Schuman, Local translation in neuronal compartments: How local is local? *EMBO Rep.* **18**, 693–711 (2017). doi: 10.15252/embr.201744045; pmid: 28404606
21. E. Kummer, N. Ban, Mechanisms and regulation of protein synthesis in mitochondria. *Nat. Rev. Mol. Cell Biol.* **22**, 307–325 (2021). doi: 10.1038/s41580-021-00332-2; pmid: 33594280
22. B. Kuzniewska *et al*., Mitochondrial protein biogenesis in the synapse is supported by local translation. *EMBO Rep.* **21**, e48882 (2020). doi: 10.15252/embr.201948882; pmid: 32558077

23. O. Bapat *et al*., VAP spatially stabilizes dendritic mitochondria to locally support synaptic plasticity. *Nat. Commun.* **15**, 205 (2024). doi: 10.1038/s41467-023-44233-8; pmid: 38177103
24. X. Wang, T. L. Schwarz, The mechanism of Ca2+ -dependent regulation of kinesin-mediated mitochondrial motility. *Cell* **136**, 163–174 (2009). doi: 10.1016/j.cell.2008.11.046; pmid: 19135897
25. J. S. Kang *et al*., Docking of axonal mitochondria by syntaphilin controls their mobility and affects short-term facilitation. *Cell* **132**, 137–148 (2008). doi: 10.1016/j.cell.2007.11.024; pmid: 18191227
26. Y. Dromard, M. Arango-Lievano, P. Fontanaud, N. Tricaud, F. Jeanneteau, Dual imaging of dendritic spines and mitochondria *in vivo* reveals hotspots of plasticity and metabolic adaptation to stress. *Neurobiol. Stress* **15**, 100402 (2021). doi: 10.1016/j.ynstr.2021.100402; pmid: 34611532
27. X. He *et al*., Gating of hippocampal rhythms and memory by synaptic plasticity in inhibitory interneurons. *Neuron* **109**, 1013–1028.e9 (2021). doi: 10.1016/j.neuron.2021.01.014; pmid: 33548174
28. N. A. Bonekamp *et al*., Small-molecule inhibitors of human mitochondrial DNA transcription. *Nature* **588**, 712–716 (2020). doi: 10.1038/s41586-020-03048-z; pmid: 33328633
29. T. C. Foster, C. M. Norris, Age-associated changes in Ca(2+)-dependent processes: Relation to hippocampal synaptic plasticity. *Hippocampus* **7**, 602–612 (1997). doi: 10.1002/(SICI)1098-1063(1997)7:6<602::AID-HIPO3>3.0.CO;2-G; pmid: 9443057
30. S. N. Burke, C. A. Barnes, Neural plasticity in the ageing brain. *Nat. Rev. Neurosci.* **7**, 30–40 (2006). doi: 10.1038/nrn1809; pmid: 16371948
31. R. Mostany *et al*., Altered synaptic dynamics during normal brain aging. *J. Neurosci.* **33**, 4094–4104 (2013). doi: 10.1523/JNEUROSCI.4825-12.2013; pmid: 23447617
32. Y. Lin *et al*., Brain activity regulates loose coupling between mitochondrial and cytosolic Ca^{2+} transients. *Nat. Commun.* **10**, 5277 (2019). doi: 10.1038/s41467-019-13142-0; pmid: 31754099
33. D. G. Wheeler *et al*., Ca(V)1 and Ca(V)2 channels engage distinct modes of Ca(2+) signaling to control CREB-dependent gene expression. *Cell* **149**, 1112–1124 (2012). doi: 10.1016/j.cell.2012.03.041; pmid: 22632974
34. Y. Wang *et al*., Chronic Neuronal Inactivity Utilizes the mTOR-TFEB Pathway to Drive Transcription-Dependent Autophagy for Homeostatic Up-Scaling. *J. Neurosci.* **43**, 2631–2652 (2023). doi: 10.1523/JNEUROSCI.0146-23.2023; pmid: 36868861
35. D. Eisner, E. Neher, H. Taschenberger, G. Smith, Physiology of intracellular calcium buffering. *Physiol. Rev.* **103**, 2767–2845 (2023). doi: 10.1152/physrev.00042.2022; pmid: 37326298
36. H. Ma *et al*., γCaMKII shuttles Ca^{2+}/CaM to the nucleus to trigger CREB phosphorylation and gene expression. *Cell* **159**, 281–294 (2014). doi: 10.1016/j.cell.2014.09.019; pmid: 25303525
37. J. M. Baughman *et al*., Integrative genomics identifies MCU as an essential component of the mitochondrial calcium uniporter. *Nature* **476**, 341–345 (2011). doi: 10.1038/nature10234; pmid: 21685886
38. D. De Stefani, A. Raffaello, E. Teardo, I. Szabò, R. Rizzuto, A forty-kilodalton protein of the inner membrane is the mitochondrial calcium uniporter. *Nature* **476**, 336–340 (2011). doi: 10.1038/nature10230; pmid: 21685888
39. M. L. Joiner *et al*., CaMKII determines mitochondrial stress responses in heart. *Nature* **491**, 269–273 (2012). doi: 10.1038/nature11444; pmid: 23051746
40. F. Fieni, D. E. Johnson, A. Hudmon, Y. Kirichok, Mitochondrial Ca2+ uniporter and CaMKII in heart. *Nature* **513**, E1–E2 (2014). doi: 10.1038/nature13626; pmid: 25254480
41. R. Yasuda, Y. Hayashi, J. W. Hell, CaMKII: A central molecular organizer of synaptic plasticity, learning and memory. *Nat. Rev. Neurosci.* **23**, 666–682 (2022). doi: 10.1038/s41583-022-00624-2; pmid: 36056211
42. J. W. Hell, CaMKII: Claiming center stage in postsynaptic function and organization. *Neuron* **81**, 249–265 (2014). doi: 10.1016/j.neuron.2013.12.024; pmid: 24462093
43. A. Hudmon, H. Schulman, Structure-function of the multifunctional Ca2+/calmodulin-dependent protein kinase II. *Biochem. J.* **364**, 593–611 (2002). doi: 10.1042/bj20020228; pmid: 11931644
44. T. Fang, K. Kasbi, S. Rothe, W. Aziz, K. P. Giese, Age-dependent changes in autophosphorylation of alpha calcium/calmodulin dependent kinase II in hippocampus and amygdala after contextual fear conditioning. *Brain Res. Bull.* **134**, 18–23 (2017). doi: 10.1016/j.brainresbull.2017.06.012; pmid: 28648815
45. N. L. Rumian, R. K. Freund, M. L. Dell'Acqua, S. J. Coultrap, K. U. Bayer, Decreased nitrosylation of CaMKII causes aging-associated impairments in memory and synaptic plasticity in mice. *Sci. Signal.* **16**, eade5892 (2023). doi: 10.1126/scisignal.ade5892; pmid: 37490545
46. C. N. Brown, K. U. Bayer, Studying CaMKII: Tools and standards. *Cell Rep.* **43**, 113982 (2024). doi: 10.1016/j.celrep.2024.113982; pmid: 38517893
47. Y. Lee *et al*., Structure and function of the N-terminal domain of the human mitochondrial calcium uniporter. *EMBO Rep.* **16**, 1318–1333 (2015). doi: 10.15252/embr.201540436; pmid: 26341627
48. E. K. Nguyen *et al*., CaMKII (Ca^{2+}/Calmodulin-Dependent Kinase II) in Mitochondria of Smooth Muscle Cells Controls Mitochondrial Mobility, Migration, and Neointima Formation. *Arterioscler. Thromb. Vasc. Biol.* **38**, 1333–1345 (2018). doi: 10.1161/ATVBAHA.118.310951; pmid: 29599132
49. P. K. Dash, B. Hochner, E. R. Kandel, Injection of the cAMP-responsive element into the nucleus of Aplysia sensory neurons blocks long-term facilitation. *Nature* **345**, 718–721 (1990). doi: 10.1038/345718a0; pmid: 2141668
50. E. R. Kandel, Y. Dudai, M. R. Mayford, The molecular and systems biology of memory. *Cell* **157**, 163–186 (2014). doi: 10.1016/j.cell.2014.03.001; pmid: 24679534
51. J. Lee *et al*., Mitochondrial cyclic AMP response element-binding protein (CREB) mediates mitochondrial gene expression and neuronal survival. *J. Biol. Chem.* **280**, 40398–40401 (2005). doi: 10.1074/jbc.C500140200; pmid: 16207717
52. H. Ryu, J. Lee, S. Impey, R. R. Ratan, R. J. Ferrante, Antioxidants modulate mitochondrial PKA and increase CREB binding to D-loop DNA of the mitochondrial genome in neurons. *Proc. Natl. Acad. Sci. U.S.A.* **102**, 13915–13920 (2005). doi: 10.1073/pnas.0502878102; pmid: 16169904
53. L. R. Bevilaqua *et al*., Experience-dependent increase in cAMP-responsive element binding protein in synaptic and nonsynaptic mitochondria of the rat hippocampus. *Eur. J. Neurosci.* **11**, 3753–3756 (1999). doi: 10.1046/j.1460-9568.1999.00830.x; pmid: 10564381
54. R. A. Schuh, T. Kristián, G. Fiskum, Calcium-dependent dephosphorylation of brain mitochondrial calcium/cAMP response element binding protein (CREB). *J. Neurochem.* **92**, 388–394 (2005). doi: 10.1111/j.1471-4159.2004.02873.x; pmid: 15663486
55. J. Pláteník *et al*., Apparent presence of Ser133-phosphorylated cyclic AMP response element binding protein (pCREB) in brain mitochondria is due to cross-reactivity of pCREB antibodies with pyruvate dehydrogenase. *J. Neurochem.* **95**, 1446–1460 (2005). doi: 10.1111/j.1471-4159.2005.03471.x; pmid: 16219034
56. D. De Rasmo, A. Signorile, E. Roca, S. Papa, cAMP response element-binding protein (CREB) is imported into mitochondria and promotes protein synthesis. *FEBS J.* **276**, 4325–4333 (2009). doi: 10.1111/j.1742-4658.2009.07133.x; pmid: 19614745
57. Y. Pan *et al*., Neuronal activity recruits the CRTC1/CREB axis to drive transcription-dependent autophagy for maintaining late-phase LTD. *Cell Rep.* **36**, 109398 (2021). doi: 10.1016/j.celrep.2021.109398; pmid: 34289350
58. T. Laviv *et al*., In Vivo Imaging of the Coupling between Neuronal and CREB Activity in the Mouse Brain. *Neuron* **105**, 799–812.e5 (2020). doi: 10.1016/j.neuron.2019.11.028; pmid: 31883788
59. S. Ahn *et al*., A dominant-negative inhibitor of CREB reveals that it is a general mediator of stimulus-dependent transcription of c-fos. *Mol. Cell. Biol.* **18**, 967–977 (1998). doi: 10.1128/MCB.18.2.967; pmid: 9447994
60. S. M. Cohen *et al*., Calmodulin shuttling mediates cytonuclear signaling to trigger experience-dependent transcription and memory. *Nat. Commun.* **9**, 2451 (2018). doi: 10.1038/s41467-018-04705-8; pmid: 29934532
61. A. T. Sørensen *et al*., A robust activity marking system for exploring active neuronal ensembles. *eLife* **5**, e13918 (2016). doi: 10.7554/eLife.13918; pmid: 27661450
62. S. S. Divakaruni *et al*., Long-Term Potentiation Requires a Rapid Burst of Dendritic Mitochondrial Fission during Induction. *Neuron* **100**, 860–875.e7 (2018). doi: 10.1016/j.neuron.2018.09.025; pmid: 30318410
63. C. I. Thomas, M. A. Ryan, N. Kamasawa, B. Scholl, Postsynaptic mitochondria are positioned to support functional diversity of dendritic spines. *eLife* **12**, RP89682 (2023). doi: 10.7554/eLife.89682.3; pmid: 38059805
64. Z. X. Fu *et al*., Dendritic mitoflash as a putative signal for stabilizing long-term synaptic plasticity. *Nat. Commun.* **8**, 31 (2017). doi: 10.1038/s41467-017-00043-3; pmid: 28652625
65. S. Arai *et al*., RGB-Color Intensiometric Indicators to Visualize Spatiotemporal Dynamics of ATP in Single Cells. *Angew. Chem. Int. Ed.* **57**, 10873–10878 (2018). doi: 10.1002/anie.201804304; pmid: 29952110
66. G. G. Gross *et al*., Recombinant probes for visualizing endogenous synaptic proteins in living neurons. *Neuron* **78**, 971–985 (2013). doi: 10.1016/j.neuron.2013.04.017; pmid: 23791193
67. Y. S. Lin, T. H. Cheng, C. P. Chang, H. M. Chen, Y. Chern, Enhancement of brain-type creatine kinase activity ameliorates neuronal deficits in Huntington's disease. *Biochim. Biophys. Acta* **1832**, 742–753 (2013). doi: 10.1016/j.bbadis.2013.02.006; pmid: 23416527
68. K. Fukumitsu *et al*., Synergistic action of dendritic mitochondria and creatine kinase maintains ATP homeostasis and actin dynamics in growing neuronal dendrites. *J. Neurosci.* **35**, 5707–5723 (2015). doi: 10.1523/JNEUROSCI.4115-14.2015; pmid: 25855183
69. R. Richter-Dennerlein *et al*., Mitochondrial Protein Synthesis Adapts to Influx of Nuclear-Encoded Protein. *Cell* **167**, 471–483.e10 (2016). doi: 10.1016/j.cell.2016.09.003; pmid: 27693358
70. D. G. Nicholls, M. W. Ward, Mitochondrial membrane potential and neuronal glutamate excitotoxicity: Mortality and millivolts. *Trends Neurosci.* **23**, 166–174 (2000). doi: 10.1016/S0166-2236(99)01534-9; pmid: 10717676
71. J. R. Friedman, J. Nunnari, Mitochondrial form and function. *Nature* **505**, 335–343 (2014). doi: 10.1038/nature12985; \pmid: 24429632
72. S. C. Cunnane *et al*., Brain energy rescue: An emerging therapeutic concept for neurodegenerative disorders of ageing. *Nat. Rev. Drug Discov.* **19**, 609–633 (2020). doi: 10.1038/s41573-020-0072-x; pmid: 32709961
73. J. R. Cardinaux *et al*., Recruitment of CREB binding protein is sufficient for CREB-mediated gene activation. *Mol. Cell. Biol.* **20**, 1546–1552 (2000). doi: 10.1128/MCB.20.5.1546-1552.2000; pmid: 10669732
74. A. Suzuki *et al*., Upregulation of CREB-mediated transcription enhances both short- and long-term memory. *J. Neurosci.* **31**, 8786–8802 (2011). doi: 10.1523/JNEUROSCI.3257-10.2011; pmid: 21677163
75. S. C. Hu, J. Chrivia, A. Ghosh, Regulation of CBP-mediated transcription by neuronal calcium signaling. *Neuron* **22**, 799–808 (1999). doi: 10.1016/S0896-6273(00)80738-2; pmid: 10230799
76. A. T. C. Lee *et al*., Association of Daily Intellectual Activities With Lower Risk of Incident Dementia Among Older Chinese Adults. *JAMA Psychiatry* **75**, 697–703 (2018). doi: 10.1001/jamapsychiatry.2018.0657; pmid: 29847678
77. A. J. Jak, The impact of physical and mental activity on cognitive aging. *Curr. Top. Behav. Neurosci.* **10**, 273–291 (2012). doi: 10.1007/7854_2011_141; pmid: 21818703
78. M. P. Blaustein, Calcium transport and buffering in neurons. *Trends Neurosci.* **11**, 438–443 (1988). doi: 10.1016/0166-2236(88)90195-6; pmid: 2469161
79. H. Ma, Q. Cai, W. Lu, Z. H. Sheng, S. Mochida, KIF5B motor adaptor syntabulin maintains synaptic transmission in sympathetic neurons. *J. Neurosci.* **29**, 13019–13029 (2009). doi: 10.1523/JNEUROSCI.2517-09.2009; pmid: 19828815
80. V. Rangaraju, N. Calloway, T. A. Ryan, Activity-driven local ATP synthesis is required for synaptic function. *Cell* **156**, 825–835 (2014). doi: 10.1016/j.cell.2013.12.042; pmid: 24529383
81. M. Levy, G. C. Faas, P. Saggau, W. J. Craigen, J. D. Sweatt, Mitochondrial regulation of synaptic plasticity in the hippocampus. *J. Biol. Chem.* **278**, 17727–17734 (2003). doi: 10.1074/jbc.M212878200; pmid: 12604600
82. Z. Li, K. Okamoto, Y. Hayashi, M. Sheng, The importance of dendritic mitochondria in the morphogenesis and plasticity of spines and synapses. *Cell* **119**, 873–887 (2004). doi: 10.1016/j.cell.2004.11.003; pmid: 15607982
83. E. Zampese *et al*., Ca^{2+} channels couple spiking to mitochondrial metabolism in substantia nigra dopaminergic neurons. *Sci. Adv.* **8**, eabp8701 (2022). doi: 10.1126/sciadv.abp8701; pmid: 36179023
84. B. Styr *et al*., Mitochondrial Regulation of the Hippocampal Firing Rate Set Point and Seizure Susceptibility. *Neuron* **102**, 1009–1024.e8 (2019). doi: 10.1016/j.neuron.2019.03.045; pmid: 31047779
85. C. J. Groten, B. A. MacVicar, Mitochondrial Ca^{2+} uptake by the MCU facilitates pyramidal neuron excitability and metabolism during action potential firing. *Commun. Biol.* **5**, 900 (2022). doi: 10.1038/s42003-022-03848-1; pmid: 36056095
86. E. Hebert-Chatelain *et al*., A cannabinoid link between mitochondria and memory. *Nature* **539**, 555–559 (2016). doi: 10.1038/nature20127; pmid: 27828947

87. B. Oettinghaus *et al*., Synaptic dysfunction, memory deficits and hippocampal atrophy due to ablation of mitochondrial fission in adult forebrain neurons. *Cell Death Differ.* **23**, 18–28 (2016). doi: 10.1038/cdd.2015.39; pmid: 25909888
88. E. L. Underwood *et al*., Enhanced presynaptic mitochondrial energy production is required for memory formation. *Sci. Rep.* **13**, 14431 (2023). doi: 10.1038/s41598-023-40877-0; pmid: 37660191
89. J. R. Gingrich *et al*., Unique domain anchoring of Src to synaptic NMDA receptors via the mitochondrial protein NADH dehydrogenase subunit 2. *Proc. Natl. Acad. Sci. U.S.A.* **101**, 6237–6242 (2004). doi: 10.1073/pnas.0401413101; pmid: 15069201
90. Y. Hirabayashi *et al*., Most axonal mitochondria in cortical pyramidal neurons lack mitochondrial DNA and consume ATP. bioRxiv, (2024).

ACKNOWLEDGMENTS

We thank X. He, L. Yan, J. Qu, and other members of the Ma laboratory for valuable discussions and insightful suggestions, and former lab members Y. Pan and S. Xie for assistance with this project. We thank S. Duan and Q. Chen for their generous help. We thank X. Pan for providing the custom-made antibody for a preliminary test. We thank the Core Facilities at Zhejiang University School of Medicine for providing technical support. **Funding:** This study was supported by the Science and Technology Innovation 2030-Major Project Grant 2021ZD0203501 (to H.M.), the National Key R&D Program of China (2019YFA0508603 to H.M.), the National Natural Science Foundation of China (grant nos. 81930030, 82230036, and 31722023 to H.M.); 31900696 to W.L.; 82271513 to B.Z.), CAMS Innovation Fund for Medical Sciences (2019-I2M-5-057 to H.M.), Project for Hangzhou Medical Disciplines of Excellence (to H.M.), Key Project for Hangzhou Medical Disciplines (to H.M.), the Fundamental Research Funds for the Central Universities of China (2023ZFJH01-01 and 2024ZFJH01-01 to H.M.), and National Institutes of Health (R01MH080047, R35NS116804 to R.Y.).
Author contributions: H.M. and W.L. conceived the project and designed the experiments. J.L. performed the electrophysiology experiments with the help of Y.C., Y.S., H.L., and K.J.; C.W. and M.D. performed the virus injection; J.L. performed immunogold electron microscopy; J.L. performed in vivo 2P imaging; M.C., L.C., and T.L. performed 2P imaging on hippocampal culture slices with the help of R.Y.; W.L. performed all the other experiments with the assistance of C.W. and the help of B.Z. and Z.G.; H.H. and T.L. helped interpret the results and guide the project. H.M. and W.L. wrote the manuscript with the help of the other authors.

Competing interests: H.M., W.L., and C.W. are inventors of a pending patent application (application number 202411263542.8) on the use of Mt-CREB as an approach for preventing brain aging. **Data and materials availability:** All data are available in the main text or the supplementary materials. The Mt-A-CREB mice are available under a material agreement with Zhejiang University.

SUPPLEMENTARY MATERIALS

science.org/doi/10.1126/science.adp6547
Materials and Methods
Figs. S1 to S9
Tables S1 to S3
References (*91*–*93*)
Movies S1 and S2

Submitted 5 April 2024; resubmitted 28 July 2024
Accepted 17 October 2024
10.1126/science.adp6547